Near-Field Measurement and Analysis of Noisy Electromagnetic Emissions: Towards Stochastic Energy-Oriented Approaches

Sidina Wane[1], Damienne Bajon[2], Johannes Russer[3], Peter Russer[3], Jean-Marc Moschetta[2],
David Thomas[4] and Gregor Tanner[4]
[1]NXP-Semiconductors, Caen-France, [2]ISAE-Université de Toulouse-France,
[3]Institute for Nanoelectronics, Technische Universität München, Germany,
[4]University of Nottingham, Nottingham, UK

Abstract — *This paper presents Near-Field measurement and analysis of Noisy Electromagnetic Emissions radiated from integrated circuits and systems. Energy-Oriented approaches suitable for stochastic signals and accounting for Field-Field correlations are proposed. Dedicated wireless Chip-to-Chip communication link and connected smart RFIC objects are used as carrier for evaluating the distribution of radiated electromagnetic fields both in the frequency-domain and the Time-Domain. Perspectives for high spatial resolution Near-Field scanning systems with controlled sensitivity and noise uncertainties are studied. Use of UAV systems as floating measurement platform are drawn with possibility of wireless powering to overcome present limitation in power-supply and energy management. Spectral and spatial responses of radiated emissions from coupled UAV and smart RFIC objects are extracted. Perspectives for the analysis of radiated emissions based on Energy Density using Multi-Resolution wavelet scalogram are drawn for the simultaneous Time-Frequency identification and localization of noisy sources.*

Index Terms —**Near-Field measurement of connected RFIC objects, IoT, MIMO, Stochastic Noise, EMC, EMI, Small cells.**

I. INTRODUCTION

The emergence of smartphones and connected objects (*e.g., Tablets, GPS, Laptops*) with the perspectives for Internet of Things (IoT) put new requirements on RFIC design, modeling and experimental verification. Today, in the conventional verification methodologies, circuit design and EM Field emission/reception are considered as disjoint and separate activities. As a consequence, mitigation of EMC/EMI issues for compliance with Power Integrity, Signal Integrity and EMC/EMI is very challenging in order to address increasing needs for higher bandwidth, lower power consumption with improved immunity to environmental uncertainties.

Near-Field measurement [1-5] appears as a bridging gap between circuit design (RFIC-Chip-Package-PCB) and field radiation (antennas) with the following driving motivations:

- Coupled analysis of spatial radiated field distributions and Spectral-domain/Time-domain responses for optimization of dynamic power management.
- Effective control/monitoring of RF performances as function of environmental uncertainties including use of MIMO and Small-cells to enhance communication capacity and coverage.

- Diagnosis of Chip-Package-PCB systems by inspection of radiated emanations for design improvement, test and root-cause analysis.

The deployment of proven Near-Field measurement solutions as a standard for the qualification of connected smart RFIC objects accounting for their environmental uncertainties requires the development of a technological plateform suitable for Noisy Stochastic [1] Signals.

In this paper, we present Near-Field measurement and analysis of radiated emissions from connected smart RFIC objects. This work is in the context of the European project NEMF21: Noisy-Electro-Magnetic-Field aware Technological Platform addressing the challenge: *Any-Device*, *Any-Network*, *Any-Where*, *Any-Time* with *Seamless Connectivity*.NEMF21 envision Chip-Package-PCB [*including antennas*] Co-Design methodologies to ensure First Time Right in the realization of 5G wireless links between systems including circuits operating as Multiple-Input-Multiple-Output devices. Experimental results for the characterization of Near-Field couplings between smartphones in presence of noisy interferers (*GPS, Tablets, Laptops, motors*) are presented.

Fig.1: Near-Field Coupling between connected Smart Objects (*interactions between smartphone, tablet and GPS devices*).

II. MAIN RESULTS, ANALYSIS AND OBSERVATIONS

II.1 Near-Field Measurement of Connected Smart RFIC Objects accounting for Environmental Uncertainties

The following experiments are conducted in various practical environmental configurations:

1) Spectral-domain characterization of radiated emissions from coupled smartphone devices as function of their separation distance in TX and RX

modes from 50MHz to 8GHz with focus on WLAN, GSM, UMTS, LTE frequency bands.

2) Spatial-domain characterization of radiated emissions from coupled smart objects (smartphone and tablet) in presence of interferers (GPS device in operation).

3) Sensitivity analysis of Near-Field probing systems as function of dynamic power levels with and without custom bypass pre-amplifier. Dedicated coupled Vivaldi antennas are designed and used as carrier for broadband evaluation of the ultimate limits of Near-Field detection sensitivity.

Different smartphone models [namely: Nexus One (*16.85-17.40dBm*), Galaxy Nexus (*15.5-16.5dBm*), Galaxy SII (*17.15dBm*), Galaxy SIII (*16.0-17.12dBm*), iPhone 4S (*17.05dBm*)] are studied in terms of their surface area and field strength emissions in front, back and side configurations. Table I below summarizes benchmarking [6] results for 5 smartphone models in terms of their surface area and the field intensity measured by the FCC (publicly available data) at the level of the antenna. The referenced Nexus model emits 13 V/m, 5.32 V/m and 10 V/m at the rear, front and side, respectively. Significant differences can already be observed which exceeds 7V/m between the front and rear emissions. 7V/m corresponds to a power density of 0.130W/m². In Tab.I, the numbers indicated in blue correspond to differences of the smartphones compared to the Nexus one for the back configuration. Fig.2 shows Illustrative overview layout showing floorplan with the approximate location of the different antennas in a smartphone (TX, TX/RX, Bluetooth and GPS).

TAB.I: BENCHMARKING DIFFERENT SMARTPHONE MODELS IN TERMS OF THEIR SURFACE AREA AND FIELD STRENGTH IN BACK, FRONT AND SIDE CONFIGURATIONS. DATA ARE PUBLICLY AVAILABLE FROM FCC.

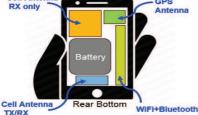| Smartphone Model	Surface Area (in cm²)	Back Field [in V/m]	Front Field [in V/m]	Side Field [in V/m]
Nexus One	71	13.0	5.32 (7.7)	10.8 (1.6)
Galaxy Nexus	92	8.44 (3.75)	4.60 (5.27)	7.3 (1.26)
Galaxy SII	71	8.97 (3.22)	4.82 (5.39)	7.84 (1.17)
Galaxy SIII	96	10.5 (1.85)	3.1 (10.6)	5.17 (6.15)
iPhone 4S	67	11.5 (1.06)	6.61 (4.8)	8.58 (2.54)

Fig. 2. Illustrative overview layout showing floorplan of the different antennas location in a smartphone (TX, TX/TX, Bluetooth and GPS).

For the spectral characterization, we consider connected smartphones in TX and RX modes as illustrated in Fig.2 with and without interferer (GPS device).

Broadband (from 50MHz to 8GHz) measured emissions are depicted in Fig.4 where UMTS, GSM and WiFi (2.4GHz) bands can be distinguished. The obtained maximum radiated emission is at 1966MHz.

Fig.3: Near-Field coupling between two smartphones with and without interferer (*GPS device in operation*).

Fig.5 shows the measured emissions radiated by the coupled smartphones with and without interferer (GPS device in operation). Radiated emissions from one single smartphone are also reported.
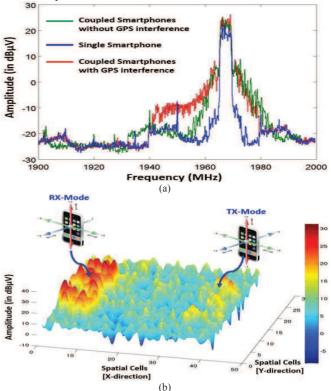

(a)

(b)

Fig.5: Measured (a) Near-Field Spectral response of radiated emissions from single smartphone and coupled smartphones with or without interferer (*GPS device in operation*). Measured (b) Near-Field spatial distribution of radiated emissions from single smartphone and coupled smartphones (*GPS device in operation*) at 1966MHz.

The coupling between connected smartphones compared to single smartphone results in significant increase (reaching more than 10dBµV) in the noise emissions. Interferences due to GPS device in operation located between the coupled smartphones extends the frequency band of the noise by 25 to

30MHz in reference to the radiation level of the coupled smartphones without interferer.Fig.6 presents the measured spatial distribution of the radiated Near-Field emissions from the coupled smartphones.
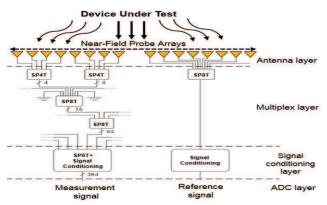

Fig.7: Principle of used Near Field scanner based on switched probe arrays operating in the frequency-band 150KHz-8GHz [7].

The spatial domain scanner consists of 1218 probes (42 in the direction of X-axis and 29 in the direction of Y-axis) that operate for frequencies between 50MHz and 8GHz. Each row and column on the scanner reference plane points to a unique probe that is spaced every 7.5mm into an electronically switched array, which results in an effective 3.75 mm spatial resolution. Electronic switches (Fig.7) are used so that the probes can sweep the entire board. Different levels of resolution can be selected. At each level, one grid is divided into four sub-grids which represents four measurement points. The highest accuracy corresponds to 120 microns spatial resolution where the maximum number of measurement points in one grid can reach 4096.

II.2 Measurement and Analysis of Radiated Emissions from Coupled UAV and Smart RFIC Objects

Unmanned Aerial Vehicles (UAVs) equipped with lightweight embedded sensors offer new potentialities for contactless measurement with the following perceived benefits:

- Use of non-stationary (mobile in remote control) floating platform for electromagnetic field probing (both Near-Field and Far Field)
- GPS (alternatively laser reflector combined with gyroplane) assisted position tracking of probing sensors with stabilization of RF-probes for accurate angle measurement on spherical contours
- Wireless data flow management when twin-UAV systems are used or with use of contactless powering in the context of outdoor applications.

Feasibility studies pushed to real implementation phases have demonstrated practical benefits of using UAVs as floating measurement platforms in diverse civilian (agriculture [8], telemetry including RF test and measurement [9]) and military (defense/security [10]) applications. However, the effective

use of UAVs as floating measurement platforms is mainly limited by battery life (autonomy) and the requirement for human interaction to deal with power management in addition to data flow management. Wireless charging (see illustration in Fig.8(a),(b)) appears as a promising solution for dealing with both challenges. Furthermore, use of UAVs for real-time measurement and probing of electromagnetic fields need proper mitigation of different noise contributors among which are couplings between motors and embedded RFIC circuitry with potential environmental uncertainties (e.g., external interferers due to outdoor moving boundary conditions).
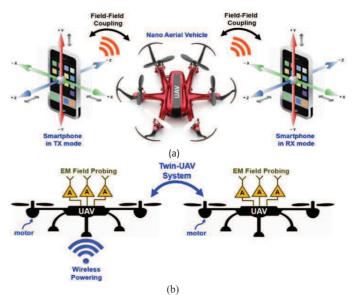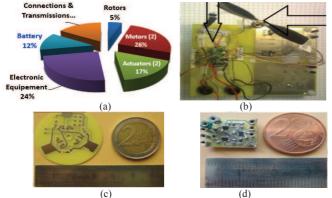

Fig.8: Coupled (a) UAV and Smart RFIC objects (e.g., smartphones): measurement and analysis of radiated electromagnetic field emissions. Wireless powering (b) of Twin-UAV system hosting EM field probing system.

A. Integration constraints for UAV systems: Co-Design Motor-RFIC circuitry

Fig.9 highlights the relative portion of RFIC circuitry in the overall weight of custom UAV developed using low-cost electronic components (including use of actuators and speed control). It clearly appears that about 50% of the assembled UAV system weight is composed of electronic circuitry with 25% contribution due to the battery used for power supply of the motors. Thus, multi-physics Electrical-Mechanical co-design is not only a requirement for Power Integrity, Signal Integrity and EMC/EMI constraints it is also a key enabler to lightweight target towards increased battery life missions. Use of MCM (Multi-Chip-Module) and SiP (System-in-Package) assembly techniques with compact laminate signal and power lines routing (Fig.9 (c),(d)) leads to reduction in payload of 30% by getting rid of wired connections. Perspectives for Chip-to-Chip communication will further reduce the weight of embedded electric systems for increased autonomy and energy savings. While power-savings are required for battery life, low power electronic systems puts strong requirement on

maximum energy levels resulting from noisy interferers which can jeopardize system functionality.

(a)   (b)

(c)   (d)

Fig.9: Estimate (a) of UAV payload weight based on custom assembly (b) built using low-cost electronic components. Module laminate-based routing for MCM and SiP assembly techniques.

Fig.10(a) shows the measured spectral response of radiated emissions by coupled UAV and smartphones with ambient noise (WiFi source).
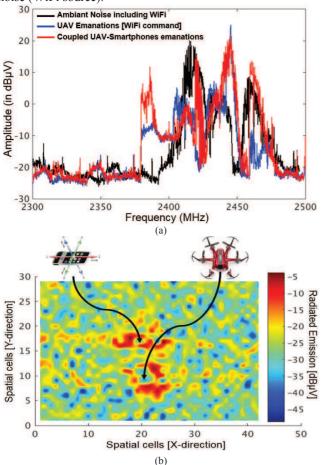

(a)

(b)

Fig.10: Measured (a) Near-Field Spectral response of radiated emissions from coupled UAV and smartphones in presence of ambient noise (*WiFi source*). Measured (b) Near-Field spatial distribution of radiated emissions from coupled UAV and smartphones in presence of ambient noise (*WiFi source*) at 2.380 MHz.

The results highlight the ambient noise level compared to the contributions of the UAV alone and the intrinsic couplings between the UAV and the smartphone. The interest for the WLAN frequency band around 2.4GHz is mainly because the UAV is controlled through a remote WiFi radio command far from the near field scanner.

Fig.10(b) presents the measured spatial distribution of the radiated Near-Field emissions from the coupled UAV and smart phone system. The spatial domain scanner consists of 1218 probes (42 in the direction of X-axis and 29 in the direction of Y-axis) that operate for frequencies between 50MHz and 8GHz.

Although frequency-domain analysis helps evaluating noise levels by inspection of the power spectrum of a signal emissions, it does not inform about the way the frequency content evolves over time. In order to overcome this limitation Multi-Resolution Wavelet-based transform can be used for simultaneous analysis in the time and frequency domains.

B. Wavelets based Multi-Resolution Energy-Oriented Analysis for Noisy Sources Localization

We define the continuous wavelet [11] transform (CWT) of a finite-energy (Hilbert space) function $R(t)$ by the following Hermitian scalar product:

$$\langle W_{b,a}(t)|R(t)\rangle = \frac{1}{\sqrt{|a|}} \int_{-\infty}^{+\infty} W_{b,a}{}^*(t)\, R(t)dt \qquad (1)$$

with:

$$W_{b,a}(t) = \frac{1}{\sqrt{|a|}} g\left(\frac{t-b}{a}\right), \text{a} \in \text{R}^+, \text{b} \in \text{R} \qquad (2)$$

where $g(t)$ is the mother wavelet.

The CWT can be understood as the correlation between the signal $R(t)$ and the wavelet atomic function $W_{b,a}(t)$.

By changing the translation parameter b assuming a constant scale a, the wavelet is sliding with a fixed bandwidth B_a and with a given center frequency ω_a along the analyzed signal.

The link between the scale a and the frequency content is made explicit by defining two frequency parameters namely the center frequency ω_0:

$$\omega_0 = \frac{1}{2\pi}\int_0^{+\infty} \omega\, |\hat{g}(\omega)|^2 d\omega \qquad (3)$$

and the bandwidth $B_0 = \sigma_\omega$ symmetrically distributed around $\omega_0.\sigma_\omega$ is given by the following expression where $\hat{g}(\omega)$ denotes the Fourier transform of $g(t$ following Parseval's theorem:

$$\sigma_\omega^2 = \frac{1}{2\pi}\int_0^{+\infty} (\omega - \omega_0)^2\, |\hat{g}(\omega)|^2 d\omega \qquad (4)$$

The scalogram of a signal $R(t)$ defined as the magnitude square of the scalar product $P_{\langle W_{b,a}|R\rangle} = \left|\langle W_{b,a}(t)|R(t)\rangle\right|^2$ represents a local Time-Frequency energy density. This energy-based representation is appropriate for analysis of transient signals with multi-scale attributes. The selection of the atomic wavelet function $g(t)$ can be based on entropy considerations [12-13]. Fig.11 presents normalized power

extracted form Fourier transform coefficients of measured near-field emissions as function of frequency with maximum energy localized around the 2.4GHz WiFi band. Use of multiscale CWT in the spectral domain [14] can be helpful especially for stochastic signals.
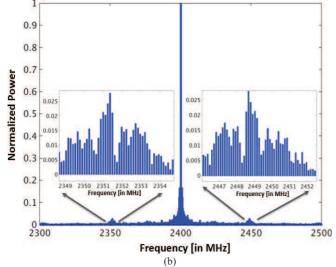

Fig.11: Normalized Power extracted from Fourier transform coefficients (b) of measured Near-Field emissions as function of frequency for coupled UAV-Smartphones.

In Fig.12, CWT is applied to the measured Near-Field emissions of coupled UAV and smartphones (reported in Fig.10) considering Morlet wavelet atomic functions [11] at different scales.

It can be practical to consider the complex Morlet wavelet as a plane wave modulated by a Gaussian envelope:

$$\psi(x) = e^{-ik_0 x} e^{-\frac{1}{2}x^2} \qquad (5)$$

The parameter k_0 is the wavenumber associated with the Morlet wavelet. The Fourier transform of the modulated Gaussian function is given by:

$$\widehat{\psi}(k) = \sqrt{2\pi} e^{-\frac{1}{2}(2\pi k - k_0)^2} \qquad (6)$$

It can be observed that $\widehat{\psi}(k = 0)$ is not vanishing which means that the mother wavelet does not satisfy the admissibility condition (mean value should be equal to zero). In order to fulfil the admissibility condition, the following corrected mother wavelet is used.

$$\psi_{corrected}(x) = \left(e^{-ik_0 x} - e^{-\frac{1}{2}k_0^2}\right) e^{-\frac{1}{2}x^2} \qquad (7)$$

The quantization of a and b leads to discrete wavelet transform with a multiresolution parameter m corresponding to a specific level associated to a sub-space V_m [11]. Such Multi-Resolution analysis of signal energy is suitable for the identification of time-varying energy flux and transient bursts not easy to detect in time- or frequency-domain descriptions [13]. Furthermore, it opens new perspectives for power and

signal integrity analysis of moving objects [15] in conjunction with Wave-oriended formulations [16].
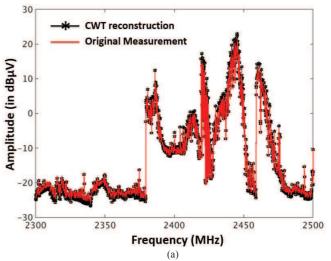

Fig.12: Comparison between Wavelet Synthesis results and original measurement.

Fig.13 shows the variation of the detected Near-Field emission as function of power applied on the DUT (switched dipole antenna) for sensitivity analysis. The measured noise floor is around -130dBm and -120dB respectively with unmatched and matched feeding lines. This noise floor is obtained using an internal Pre-amplifier. It appears clearly that the indirect coupling/matching can affect the noise floor within -10dBm variation.
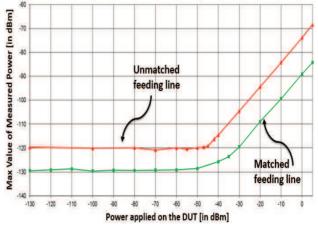

Fig.13: Measured Near-Field radiated emission from as function of input power levels using switched dipole antenna as DUT.

III. CONCLUDING REMARKS AND LOOK-AHEAD

Experimental characterization of radiated emissions from coupled UAV and smart RFIC Objects in presence of noisy interferers have been presented. Spectral and spatial responses of radiated emissions from coupled smartphones are extracted in *TX* (Transmit) and *RX* (Receive) modes with focus on WLAN frequency bands. The obtained experimental characterization results pave the way towards EMC/EMI,

Power Integrity and Signal Integrity aware design and verification of nomad connected objects. The sensitivity of the Near-Field measurement is assessed as function of input power levels ranging from +5dBm to -130dBm using switched dipole antenna integrated on laminate substrate. The ultimate sensitivity limit is evaluated to be around -130dBm which drops to –120dBm with load mismatch/coupling. Measurement results for the characterization of Near-Field couplings between smartphones in presence of UAV reveal non negligible interference levels resulting from couplings between UAV motors and the RFIC circuitry (e.g., smartphones, GPS, gyros). These interferences can limit the sensitivity of embedded Near-Field probes when UAV systems are used as remote floating platform for test and measurement purposes. Multi-Resolution Wavelet-based Energy-oriented approaches [16] are proposed in the perspectives of Multi-Physics Time-Frequency Co-Analysis. The selection of the best atomic wavelet function shall be studied both for stationary and non-stationary signals based on entropy considerations. The European project NEMF21 technological plateform will open perspectives for proper characterization of RFIC nomad objects by handling power spectral densities for stochastic noisy signals instead of conventional voltage and current amplitudes.

ACKNOWLEDGMENT

REFERENCES

[1] A. Russer and Peter Russer "Modeling of Noisy EM Field Propagation Using Correlation Information" in *IEEE Trans. on Microwave Theory and Tech*., vol. 63, No. 1, pp 76-89, 2015.

[2] J. A. Russer, G. Gradoni, G. Tanner, S. C. Creagh, D. Thomas, C. Smartt, and P. Russer, "Evolution of transverse correlation in stochastic electromagnetic fields," in IEEE MTT-S Int. Microwave Symposium (IMS), 2015, May 2015, pp. 1–3.

[3] X Tong, D W. P. Thomas, A Nothofer, P Sewell, and C Christopoulos, "*Modeling Electromagnetic Emissions From Printed Circuit Boards in Closed Environments Using Equivalent Dipoles*" IEEE Transactions on Electromagnetic Compatibility,Vol. 52, NO. 2, MAY 2010 pp 462-470.

[4] J.A Russer, N. Uddin, A.S. Awny, A. Thiede, P. Russer, "*Near-Field Measurement of Stochastic Electromagnetic Fields*", IEEE Electromagnetic Compatibility Magazine, Pages: 79 - 85, Volume: 4, Issue: 3, 2015.

[5] A. Baev, A. Gorbunova, M. Konovalyuk, Y. Kuznetsov, and J. A. Russer, "*Stochastic EMI sources localization based on ultra wide band Near-Field measurements*," in European Microwave Conference (EuMC), Nuremberg, 6-10 Oct. 2013, pp. 1131-1134.

[6] B. Distl, F. Legendre, "*Are Smartphones Suited for DTN Networking*?", 13th International Symposium on Modeling and Optimization in Mobile, Ad Hoc, and Wireless Networks (WiOpt),2015, pp.90-95.

[7] http://www.electronicinstrument.com/em2012.pdf.

[8] Zhang, C. and Kovacs, J. M.: "*The application of small unmanned aerial systems for precision agriculture: a review*", Precis. Agric., 13, 693–712, doi: 10.1007/s11119-012-9274-5, 2012.

[9] E. Yanmaz, R. Kuschnig, and C. Bettstetter, "*Channel measurements over 802.11a-based UAV-to-ground links*," in Proc. IEEE Global Commun. Conf. (GLOBECOM), pp. 1280–1284, 2011.

[10] Moschetta, Jean-Marc *The aerodynamics of micro air vehicles: technical challenges and scientific issues.* Internation Journal of Engineering Systems Modelling and Simulation, vol. 6 (n° 3/4). pp. 134-148. ISSN 1755-9758, 2014.

[11] S. Mallat, "*A Wavelet Tour of Signal Processing*", 3rd ed. New York: Academic Press, 2009.

[12] Coifman, R.R.; M.V. Wickerhauser (1992), "*Entropy-based Algorithms for best basis selection*," *IEEE Trans. on Inf. Theory*, vol. 38, 2, pp. 713–718, 1992.

[13] N. D. Kelley, R. M. Osgood, J. T. Bialasiewicz, and A. Jakubowski, "*Using wavelet analysis to assess turbulence/rotor interactions*," *Wind Energy*, vol. 3, no. 3, pp. 121–134, Jul. 2000.

[14] A. Di Falco, T. F. Krauss, and A. Fratalocchi, "*Lifetime statistics of quantum chaos studied by a multiscale analysis*". Appl. Phys. Lett. 100, 184101 (2012).

[15] S. Wane, O. Doussin, D. Bajon, J. Russer and P. Russer, "*Stochastic Approach for Power Integrity, Signal Integrity, EMC and EMI Analysis of Moving Objects*", pp. 1554-1557, ICEAA 2015.

[16] S. Wane, "*Power Integrity, Signal Integrity, EMI & EMC in Integrated Circuits and Systems: Towards Multi-Physics Energy-Oriented Approaches*," Habilitation à Diriger des Recherches, 2013.